

Fully gapped superconductivity in SrNi₂P₂

Nobuyuki Kurita^{1,2}, Filip Ronning¹, Corneliu F. Miclea¹, Eric D. Bauer¹, Krzysztof Gofryk¹, J. D. Thompson¹, Roman Movshovich¹

¹Los Alamos National Laboratory, Los Alamos, New Mexico 87545, USA

²National Institute for Materials Science, Tsukuba, Ibaraki 305-0003, Japan

(Dated: July 22, 2018)

We investigated the superconducting gap structure of SrNi₂P₂ ($T_c = 1.4$ K) via low-temperature magneto-thermal conductivity $\kappa(T, H)$ measurements. Zero field thermal conductivity κ decreases exponentially $\kappa \propto \exp(-aT_c/T)$ with $a = 1.5$, in accord with the BCS theory, and rolls over to a phonon-like $\kappa \propto T^3$ behavior at low temperature, similar to a number of conventional s -wave superconductors. In addition, we observed a “concave” field dependence of the residual linear term $\kappa_0(H)/T$. These facts strongly rule out the presence of nodes in the superconducting energy gap of SrNi₂P₂. Together with a fully gapped Fermi surface in the superconducting state of BaNi₂As₂ ($T_c = 0.6 - 0.7$ K), demonstrated in our recent work, these results lead us to stipulate that fully gapped superconductivity is likely to be a universal feature of Ni-based pnictide superconductors.

PACS numbers: 74.70.Dd, 74.25.Fy, 74.25.Op

I. INTRODUCTION

Since the discovery of superconductivity in LaFeAs(O,F),¹ one of the so-called Fe-pnictides, a considerable number of experimental and theoretical investigations have been performed on this class of materials, which includes compounds with high superconducting transition temperatures (T_c) up to ~ 56 K,²⁻⁴ in proximity to magnetism accompanied by structural transitions, and in a variety of crystal structures which share FePn layers ($Pn = \text{As, P, Se}$ etc.).⁵ The important issue of the superconducting pairing symmetry in Fe-pnictides is still controversial. Conclusions for the gap structure range from a single s -wave-like gap,⁶ to multiple gaps,⁷ to the existence of nodes in the gap, depending not only on the probe used to make the measurement, but also on a particular sample composition.⁸⁻¹⁰ Consequently, the gap function in Fe-pnictides is proposed to be dependent on the structure of the Fermi surface and to be non-universal.¹¹ Theoretically, a sign-reversing s_{\pm} model, based on the unique Fermi surfaces in Fe-pnictides,¹²⁻¹⁵ was proposed by several groups to resolve many apparent experimental discrepancies.¹⁶ Investigations of the related families of compounds may help to resolve the issue of the superconducting gap symmetry and the origin of the pairing mechanism in Fe-pnictides.

Ni-analogs (Ni-pnictides), with the same structure as Fe-pnictides, also superconduct.¹⁷⁻²⁵ In addition, some Ni-pnictides share several properties with Fe-pnictides, such as structural transitions from tetragonal to a lower symmetry crystal lattice,^{24,25} enhancement of T_c by doping,^{26,27} and the importance of low-dimensionality for achieving higher T_c .^{25,28} On the other hand, there are crucial differences including the magnitude of T_c , which does not exceed 5 K in any of the Ni-based compounds, the absence of magnetic ordering,²⁵ and a more three dimensional structure of the Fermi surface in Ni-pnictides.²⁹ Correlating the commonalities and, more im-

portantly, the differences in physical properties between Fe- and Ni-pnictides could hold important clues to, in particular, the origin of the high T_c in Fe-pnictides.

In our recent thermal conductivity κ and specific heat C studies of BaNi₂As₂,³⁰ with $T_c = 0.7$ K and a structural transition $T_0 = 130$ K,²⁴ we have established fully gapped superconductivity in this Ni-pnictide. Similar conclusions were recently arrived at for LaNiAs(O,F) via nuclear quadrupole resonance (NQR) measurements.³¹ While the electronic structure for various Ni-pnictides are qualitatively similar,^{29,32-34} the detailed differences between them allow us to check for universality of the superconducting properties. Here, we report a thermal conductivity study of another Ni-pnictide, SrNi₂P₂ ($T_0 = 325$ K, $T_c = 1.4$ K).²⁵ Low-temperature thermal transport is an established powerful tool for investigating superconducting properties. In particular, the low-temperature magnetic field dependence of the thermal conductivity κ is instructive to detect whether the Fermi surface is fully gapped in the superconducting state^{30,35-40} or there are nodes in the gap.^{41,42} Thermal conductivity of SrNi₂P₂ reported here is qualitatively similar to that of BaNi₂As₂, which leads us to suggest that fully gapped superconductivity might be a universal feature in Ni-pnictides, as opposed to a large variation in a gap structure observed in Fe-pnictides.

II. EXPERIMENTAL DETAILS

SrNi₂P₂ forms in the ThCr₂Si₂-type tetragonal structure. Single crystal samples were grown in Sn flux as described in previous reports.^{25,43} Thermal conductivity measurements were performed via standard one-heater-two-thermometers technique on a plate-like crystal ($\sim 2 \times 1 \times 0.3$ mm³) in a range of 50 mK to 3 K using an S.H.E. corp.’s dilution refrigerator equipped with a 9 T superconducting magnet. The heat current q was

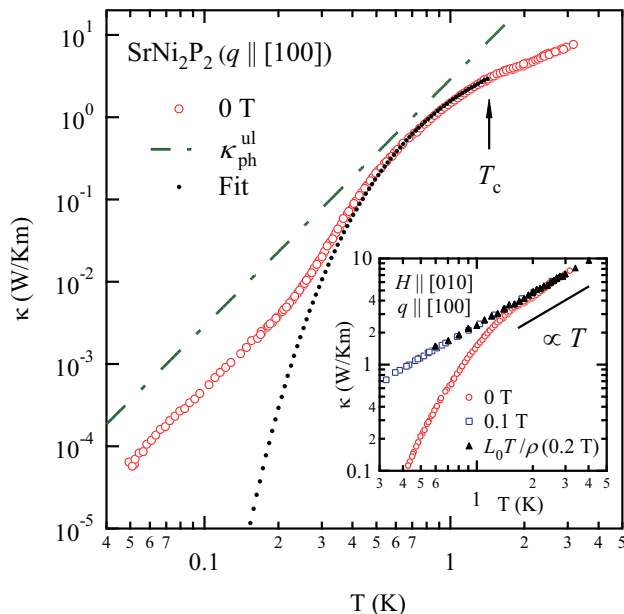


FIG. 1: (Color online) Main figure: Temperature dependence of the thermal conductivity $\kappa(T)$ of SrNi_2P_2 in zero field for a heat current $q \parallel [100]$, on a double logarithmic plot. An arrow indicates T_c ($=1.4$ K), determined from the resistivity and specific heat data. A dotted curve shows a fit to $\kappa(T)$ with a BCS curve defined as $\kappa = C \exp(-aT_c/T)$. A dashed-dotted line represents the calculated upper limit of the phonon conductivity $\kappa_{\text{ph}}^{\text{ul}} (\propto T^3)$ based on the scattering off the sample boundary. Inset: measured (open symbols) and estimated electronic thermal conductivity in normal state (solid triangles). A straight line is a guide to the eye for $\kappa \propto T$. Applied field $H \parallel [010]$, and the heat current $q \parallel [100]$.

applied along $[100]$, the longest dimension of the sample. Pt wires, spot-welded to the sample, provided thermal links to the heater, thermometers, and the bath. Meanwhile, superconducting NbTi wires provided electrical connection to the heater and RuO_2 thermometers, while thermally isolating them from the support frame. Electrical resistivity was measured down to 0.4 K in a physical property measurement system (PPMS: Quantum Design), using the crystal (with the same electrical contacts) that was used in thermal conductivity measurements. Magnetic field was always applied along the second longest dimension of the sample (within the plate), $H \parallel [010]$, resulting in a $H \perp q$ arrangement. Measurements were performed upon field cooling from above T_c to achieve a uniform magnetic flux distribution. Magnetic field history dependence was explored in a separate set of experiments described below.

III. RESULTS

Figure 1 shows the temperature dependence of thermal conductivity $\kappa(T)$ of SrNi_2P_2 in zero field for

the heat current $q \parallel [100]$. In the normal state, as shown in the inset of Fig. 1, $\kappa(T)$ follows an approximately T -linear variation both above T_c in zero field and in the whole temperature range measured in a field of 0.1 T ($\gg H_{c2}(0) = 0.039$ T²⁵). Solid triangles represent the electronic conductivity κ_e in the normal state, estimated from resistivity via the Wiedemann-Franz law: $\kappa_e = L_0 T / \rho$, with the Lorenz number $L_0 = 2.44 \times 10^{-8}$ W Ω /K². Good agreement between the measured κ and the estimated κ_e in the normal state in fields above H_{c2} implies that the heat transport in the normal state of SrNi_2P_2 is dominated by the electrons, and the phonon conductivity is negligible. In the superconducting state below T_c , $\kappa(T)$ follows an exponential form ($\sim \exp(-aT_c/T)$, expected from the BCS theory, with $a = 1.5$ down to 0.5 K, as indicated by the dotted curve). Below 0.5 K, $\kappa(T)$ starts to deviate from the exponential T -dependence and, below 0.3 K, it follows a power law T^α dependence, with $\alpha = 3$. A $\kappa \propto T^\alpha$ behavior, with $2 < \alpha < 3$, has been reported in a number of conventional s -wave superconductors, and is commonly attributed to a dominant phonon conductivity, κ_{ph} . κ_{ph} can overcome the exponentially-reduced κ_e at low-temperature, even when $\kappa_{\text{ph}} \ll \kappa_e$ in the normal state, as in SrNi_2P_2 . The upper limit of the phonon thermal conductivity $\kappa_{\text{ph}}^{\text{ul}} (\propto T^3)$ is determined by the scattering off the sample boundaries.⁴⁴ In fact, using the coefficient $\beta = 4.6$ J/K⁴ m³ of the low temperature T^3 term of the phonon specific heat, mean phonon velocity, $\langle v \rangle = 3 \times 10^3$ m/s²⁵, and the phonon mean free path $l_{\text{ph}}^{\text{ul}} = \sqrt{4ab/\pi} = 6.3 \times 10^{-4}$ m, with the dimensions $a = 1.2$ mm and $b = 0.3$ mm of the sample cross-section, we obtain $\kappa_{\text{ph}}^{\text{ul}} = \frac{1}{3} \beta T^3 \langle v \rangle l_{\text{ph}} = 2.9 \times T^3$ W/K⁴ m, shown by a dashed-dotted line in the main panel of Fig. 1. This estimate is large enough to account for the T^3 variation of the low-temperature conductivity, and the discrepancy between the estimate and experimental data indicates an additional scattering mechanism, which reduces the phonon mean free path below the value above determined by the sample cross-section.

The thermal conductivity of SrNi_2P_2 displays features common to other conventional s -wave superconductors and BaNi_2As_2 . In figure 2 we compare κ vs T/T_c in zero field for SrNi_2P_2 , BaNi_2As_2 (#1, $T_c = 0.68$ K),³⁰ BaNi_2As_2 (#2, $T_c = 0.62$ K),⁴⁵ and the s -wave superconductor Al.^{44,46} Despite widely varying absolute values, the overall temperature variation of $\kappa(T)$ in SrNi_2P_2 and in another Ni-pnictide BaNi_2As_2 resembles that of a number of conventional s -wave superconductors, e.g. Al, in terms of (i) a T -linear variation due to electrons in the normal state, (ii) a BCS-like $\exp(-aT_c/T)$ behavior with $a \sim 1.3$ -1.5 in the superconducting state below T_c ,^{44,47} and (iii) a T^α -dependence with $\alpha = 2$ -3 in the lowest temperature region. In contrast, $\kappa(T)$ of Fe-pnictides exhibits a distinct rise when the sample enters the superconducting state.⁴⁸⁻⁵¹ The rise at T_c in $\kappa(T)$ in Fe-pnictides superconductors is reminiscent of thermal conductivity in high- T_c cuprates⁵² and in heavy fermion

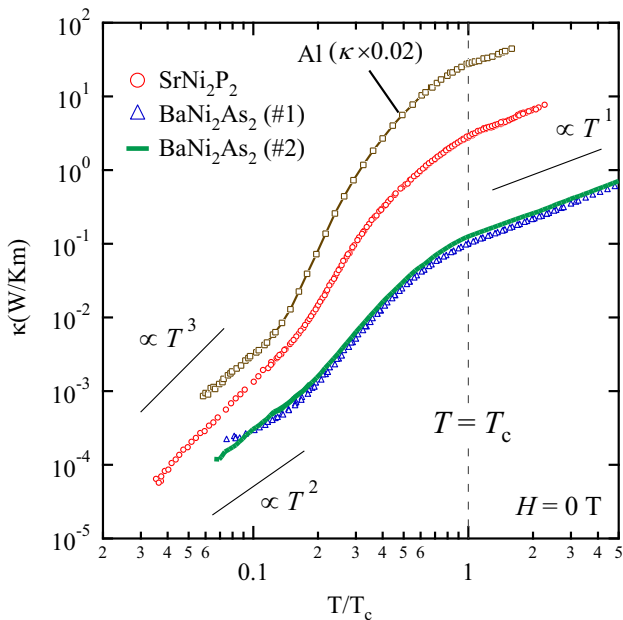


FIG. 2: (Color online) Comparison of zero-field κ vs T/T_c in SrNi_2P_2 , BaNi_2As_2 (#1, $T_c = 0.68$ K),³⁰ BaNi_2As_2 (#2, $T_c = 0.62$ K),⁴⁵ and a conventional s -wave superconductor Al ($T_c = 1.2$ K).⁴⁶ For Al, κ is multiplied by 0.02. Solid lines are guides-to-the-eye representing $\kappa \propto T^n$ ($n = 1, 2, 3$).

compounds, such as CeCoIn_5 ,⁵³ which is a result of a remarkable increase of the electronic mean free path in the superconducting state that overwhelms the reduction in the density of states.

Next, we turn to the magnetic field dependence of the low-temperature thermal conductivity in SrNi_2P_2 . The magnetic field dependence of the residual linear term $\frac{\kappa_0}{T}/\frac{\kappa}{T}|_{T \rightarrow 0}$ has been used in the past (e.g. in the case of BaNi_2As_2) to identify the structure of the superconducting gap symmetry. Namely, a concave ($\propto \sqrt{H} \exp(-b\sqrt{H}H_{c2}/H)$) dependence of the residual linear term at low magnetic fields indicates a fully gapped Fermi surface in the superconducting state, while a convex ($\propto \sqrt{H}$) field dependence indicates the presence of node(s) in the energy gap. Figure 3(a) shows κ/T vs T of SrNi_2P_2 in several fields up to 100 mT for $H \parallel [010]$ and $q \parallel [100]$. With the application of magnetic fields, κ/T continuously increases and saturates above H_{c2} . From the thermal conductivity data, we determine $H_{c2} \sim 40$ mT, in a good agreement with H_{c2} determined from the specific heat data.²⁵ The rise of conductivity with field can only be attributed to the electronic contribution. As magnetic field is applied, the phonon thermal conductivity is either suppressed due to additional scattering from the vortices in the mixed state, or it is approximately constant when the phonon mean free path is smaller than the distance between the pinned vortices. In contrast to the case in BaNi_2As_2 , where the low-temperature κ/T can be expressed as $a + bT^2$ in the in-

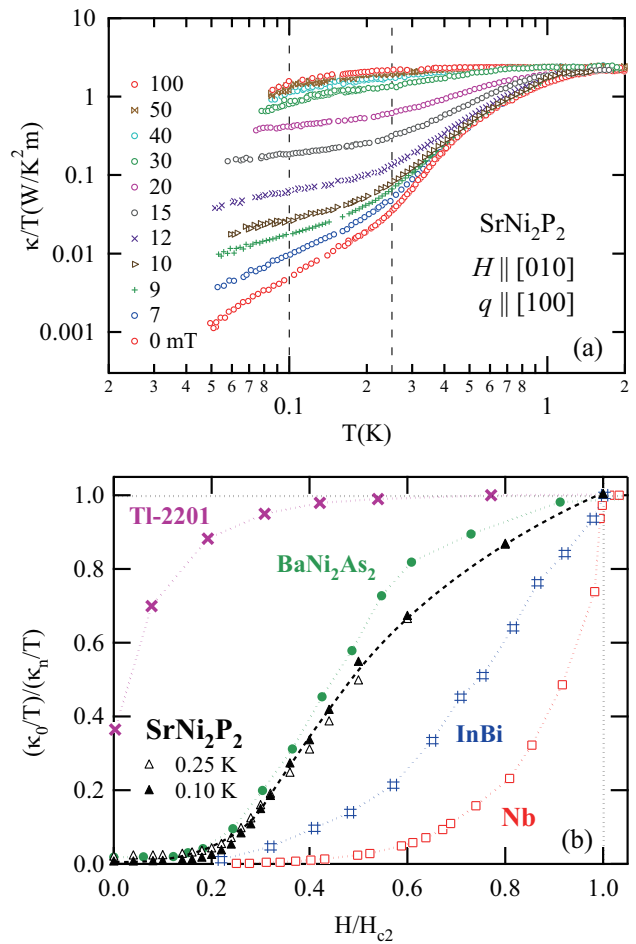


FIG. 3: (Color online) (a) κ/T vs T of SrNi_2P_2 in several fields up to 100 mT for $q \parallel [100]$ and $H \parallel [010]$. Dashed vertical lines correspond to $T = 0.10$ K and 0.25 K, at which conductivity at different fields were determined for panel (b). (b) Thermal conductivity at 0.10 K and 0.25 K, divided by the normal state value, $(\kappa_0/T)/(\kappa_n/T)$, of SrNi_2P_2 as a function of H/H_{c2} . The data for fully gapped superconductors in the clean³⁵ (Nb) and the dirty³⁶ limit (InBi and BaNi_2As_2), and a nodal superconductor $\text{Tl}_2\text{Ba}_2\text{CuO}_{6+\delta}$ (Tl-2201)⁴² are displayed for comparison. Dotted lines are guides to the eye.

vestigated field region, the low-temperature κ of SrNi_2P_2 cannot be expressed as T^α with a field-independent parameter α . The variation of α with field may be ascribed to the change in the ratio of electronic and phononic conductivity with field. We therefore used the variation of the measured $(\kappa(T)/T)/(\kappa_n/T)$ at a finite low temperature as a function of field to observe the effect of the excited quasiparticles.

The field dependence of the scaled thermal conductivity of SrNi_2P_2 at 0.1 K and 0.25 K ($\ll T_c$) is shown in Fig. 3(b) as $(\kappa_0/T)/(\kappa_n/T)$ vs H/H_{c2} for $H \perp q$, where the normal state value κ_n is obtained at 0.1 T. Data for Nb,³⁵ InBi,³⁶ and $\text{Tl}_2\text{Ba}_2\text{CuO}_{6+\delta}$ (Tl-2201)⁴² are shown for comparison as representative examples of a clean s -

wave superconductor, a dirty s-wave superconductor, and a d -wave superconductor, respectively. A concave field dependence, clearly observed for Nb in the clean limit, is a consequence of states initially localized within the vortex cores becoming delocalized as the wave-functions increasingly overlap between neighboring vortices as the vortex density increases with magnetic field. In the dirty limit (InBi), where the magnitude of the superconducting gap is reduced by impurities, the field evolution becomes more gradual below H_{c2} , but remains concave in the low field regime. In contrast, $(\kappa_0/T)/(\kappa_n/T)$ of a nodal superconductor such as Tl-2201⁴² has a substantial residual value in zero field and displays a convex field dependence due to the Volovik effect.⁵⁴ In our recent work,³⁰ we concluded that BaNi₂As₂ (also shown for comparison) is a fully gapped superconductor from the relatively fast but concave field dependence of κ_0/T in the low-field region. We also established that our BaNi₂As₂ samples were in the dirty limit as the estimated mean free path, $l_e = 70 \text{ \AA}$, was much smaller than the coherence length, $\xi = 550 \text{ \AA}$.³⁰ The data for SrNi₂P₂ is remarkably similar to BaNi₂As₂. The value of $(\kappa_0/T)/(\kappa_n/T)$ at 0.1 K is negligibly small (4×10^{-3}) in zero field, and the field dependence is concave at low fields. Thus, we conclude that SrNi₂P₂ is a fully gapped superconductor in the dirty limit. As in BaNi₂As₂, $\kappa_0/T(H)$ of SrNi₂P₂ exhibits a slight shoulder close to $H/H_{c2} = 1$. This could be due to a distribution of H_{c2} in the crystal, or multiband superconductivity which gives rise to a similar field dependence.^{39,40} However, interband scattering in these dirty samples should wipe out the effects of multiband superconductivity.

Fully gapped superconductivity in SrNi₂P₂ is also suggested by the comparison of the specific heat data with that of BaNi₂As₂ in zero field. Figure 4 shows the normalized C/T with respect to normalized T/T_c for SrNi₂P₂ and BaNi₂As₂. Both sets of data, which overlap almost perfectly, can be fit with a BCS curve with a slightly smaller energy gap ($\Delta = 1.61 k_B T_c$) than that for weak coupling ($\Delta = 1.76 k_B T_c$). This is in contrast to the nodal superconductor Sr₂RuO₄,⁵⁵ which has a smaller jump at T_c and, more importantly, much higher density of low energy excitations at low temperature. The data from an Fe-pnictide BaFe_{1.84}Co_{0.16}As₂ with $T_c = 20 \text{ K}$ ⁵⁶ is qualitatively similar to that of the Ni-pnictides in Fig. 4. However, a larger specific heat jump indicates that a larger gap over some portions of the Fermi surface is required, while the larger specific heat at the lowest temperatures indicates that a smaller gap on other portions is required. Consequently, a superconducting gap which varies significantly around the Fermi surface is required to explain the heat capacity data of Ba(Fe,Co)₂As₂.⁵⁶⁻⁶⁰ Interestingly, although it is a significantly smaller effect, similar systematic deviations can be seen between the Ni-pnictide data and the single gap BCS fit. This indicates that weak multi-gap behavior might also be present in the Ni-pnictides, although not nearly as pronounced as in the Fe-pnictides.

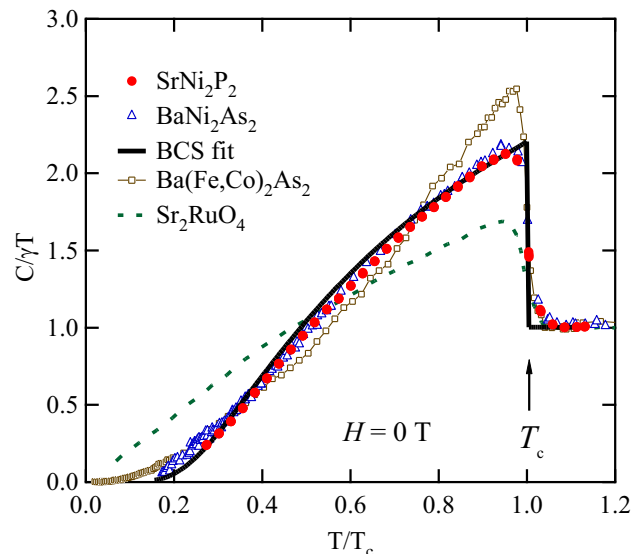


FIG. 4: (Color online) Scaled specific heat versus temperature for SrNi₂P₂, BaNi₂As₂,³⁰ Sr₂RuO₄ - an unconventional superconductor with comparable T_c ,⁵⁵ and an Fe-pnictide BaFe_{1.84}Co_{0.16}As₂ with $T_c = 20 \text{ K}$.⁵⁶ Solid curve represents a theoretical calculation based on weak coupling BCS superconductivity with a slightly smaller energy gap. The BaFe_{1.84}Co_{0.16}As₂ data has had the phonon contribution and a residual linear term subtracted.

IV. DISCUSSIONS

The thermal conductivity data presented here for Ni-pnictides display qualitatively similar behavior to that found in several Fe-based superconductors. In Fe-pnictides, a more rapid concave field dependence of the residual linear term than observed here has been attributed to a highly anisotropic gap.⁶¹⁻⁶⁵ Yet other studies of different compositions observe a finite residual linear term with a convex field dependence, which is attributed to nodal superconductivity.^{11,66,67} Our data indicate that SrNi₂P₂ (and BaNi₂As₂) are fully gapped single (perhaps very weakly anisotropic) gap superconductors. NQR results on LaNiAs(O,F) and Fe-pnictides are consistent with the differences observed in thermal transport. A Hebel-Schlichter peak is observed in $1/T_1$ in LaNiAs(O,F) followed by an exponential decay, consistent with a fully gapped s-wave superconductor,³¹ while $1/T_1$ in the Fe-based materials shows evidence for a strongly k -dependent gap.^{8,9} The differences between the Fe- and Ni-based superconductors could originate from their contrasting Fermi surfaces, quasi-two-dimensional in the former, while more complicated and three-dimensional in the latter.^{28,29,68-70} A recent X-ray spectroscopy plus DMFT study suggests that LaNiAsO is more strongly correlated than LaFeAsO,⁷¹ although this seems to contradict the results of thermopower⁷² and optical conductivity.⁷³ From thermal transport studies on BaNi₂As₂ and SrNi₂P₂, the superconductivity

in Ni-pnictides is most likely conventional phonon mediated s -wave pairing, while the issues of the pairing mechanism and the gap symmetry are still controversial in Fe-pnictides. The fact that the two iso-structural Ni-pnictide superconductors discussed here show fully gapped Fermi surfaces is most noteworthy, since two out of their three constituents are different. In particular, As and P were shown to lead to a different character of magnetic fluctuations in Fe-pnictide compounds⁷⁴. Our results, however, indicate that substituting Fe with Ni is by far the most important aspect of the Ni-pnictide superconductors, leading to qualitatively different character (and likely the origin) of superconductivity with fully gapped Fermi Surface.

Finally, we want to draw attention to the high sensitivity of thermal conductivity data in SrNi₂P₂ to a cooling/field variation route used to reach the initial state of the experimental run. Figure 5 shows $\kappa(T)$ of SrNi₂P₂ obtained for zero-field cool (ZFC) and field cool (FC) sample at (a) 10 mT and (b) 15 mT. For both fields the ZFC and FC data are markedly different. The 10 mT ZFC data almost coincides with the zero field data, while the 15 mT ZFC data is very close to the 11 mT FC data. Above 20 mT, the difference between the ZFC and FC $\kappa(T)$ data (not shown) is no longer detectable. Note that, as indicated by arrows in the inset of Fig. 5(b), the ZFC 15 mT $\kappa(T)$ deviates from FC 11 mT data around a characteristic temperature $T_1^* = 0.4$ K and merges the FC 15 mT data around $T_2^* = 0.7$ K ($< T_c$). We interpret this behavior in the following way: below T_1^* the magnetic flux in the 15 mT ZFC run is frozen, and its effect on the heat transport is identical to that in the 11 mT FC sample. Above T_1^* additional flux begins to penetrate into the sample, and the flux distribution becomes indistinguishable (via thermal conductivity measurement) from that in the FC sample at the same field (15 mT) above T_2^* . Similar differences were found for fields up to 20 mT although the difference between FC and ZFC data becomes smaller with increasing field (not shown). Such field hysteresis is often observed in superconductors with strong magnetic flux pinning. Based on the Bean model,⁷⁵ which phenomenologically describes irreversible superconducting properties, in the case of zero field cooling magnetic flux begins to enter the sample from the edges, the penetration distance being proportional to the applied field in a low-field region. In the normal state magnetic field uniformly penetrates the sample, and therefore in a FC sample the flux distribution is uniform, and its thermal conductivity always represents an upper limit for that in the ZFC sample at the same field. This model therefore can explain the magnetic field history dependence of thermal conductivity of SrNi₂P₂ described above. However, it is also expected from that model that when a sample is cooled in a magnetic field greater than H_{c2} , and the field is then ramped down to the experimental field H_{exp} within the superconducting phase, a substantial extra flux should exist in the sample compared to the FC case for the same field

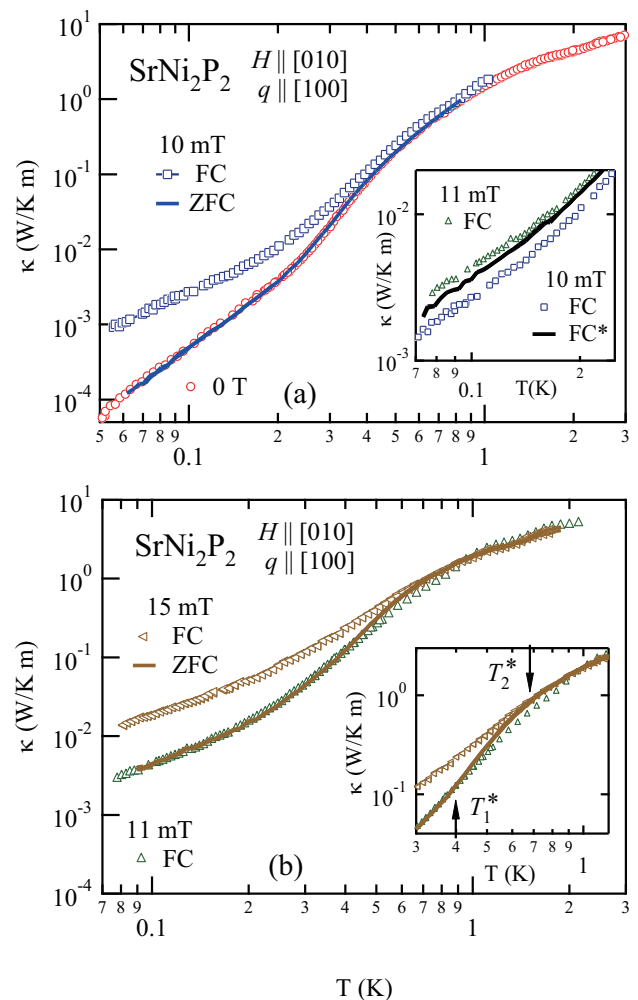


FIG. 5: (Color online) κ vs T of SrNi₂P₂ for different system preparation, zero-field cooling (ZFC) and field-cooling (FC), at (a) 10 mT and (b) 15 mT. Insets: (a) comparison of FC and FC* data for 10 mT, and the data at 11 mT (FC). FC* at 10 mT data was collected after cooling the sample in a field above H_{c2} , and then ramping it down to the measurement field. (b) Zoomed in κ vs T . 15 mT ZFC data deviates from 11 mT data at (T_1^*), and merges with 15 mT FC data (T_2^*), as indicated by the arrows.

H_{exp} . However, the effect of such trapped flux although present is smaller than expected in SrNi₂P₂: as seen in the inset of Fig. 5(a), the FC* data, obtained by cooling the sample in a field of 100 mT ($\gg H_{c2}$) and then reducing the field to 10 mT at the lowest temperature, is rather close to the 10 mT FC data, and just below the 11 mT FC data, indicating a difference in the energy barriers for flux to enter and leave the sample. The observed strong field history dependence of thermal conductivity emphasizes the need for field cooled experiments, especially when one attempts to determine the symmetry of the superconducting gap from the field dependence of the low temperature properties.

V. CONCLUSION

To conclude, we have performed magneto-thermal conductivity experiments on SrNi_2P_2 to identify the structure of the superconducting gap. Both from the temperature and field dependence of thermal conductivity, we conclude that SrNi_2P_2 is a fully gapped superconductor, as is the case in BaNi_2As_2 . We stipulate that the fully gapped spectrum might be a universal feature in Nipnictides. In addition, we found a substantial field history dependence of the thermal conductivity of SrNi_2P_2 ,

which raises a note of caution for experiments done in magnetic field in this family of compounds.

Acknowledgment

We would like to thank I. Vekhter and L. Civale for useful discussions. Work at Los Alamos National Laboratory was performed under the auspices of the US Department of Energy, and supported in part by the Los Alamos LDRD program.

-
- ¹ Y. Kamihara, T. Watanabe, M. Hirano, and H. Hosono, *J. Am. Chem. Soc.* **130**, 3296 (2008).
- ² H. Kito, H. Eisaki, and A. Iyo, *J. Phys. Soc. Jpn.* **77**, 063707 (2008).
- ³ Z. -A. Ren, W. Lu, J. Yang, W. Yi, X. -L. Shen, Z. -C. Li, G. -C. Che, X. -L. Dong, L. -L. Sun, F. Zhou, and Z. -X. Zhou, *Chin. Phys. Lett.* **25**, 2215 (2008).
- ⁴ C. Wang, L. Li, S. Chi, Z. Zhu, Z. Ren, Y. Li, Y. Wang, X. Lin, Y. Luo, S. Jiang, X. Xu, G. Cao, Z. Xu, *Europhys. Lett.* **83** 67006 (2008).
- ⁵ For recent reviews, see, K. Ishida, Y. Nakai, and H. Hosono, *J. Phys. Soc. Jpn.* **78**, 062001 (2009), D. C. Johnston, *Advances in Physics* **59**, 803 (2010), Y. Mizuguchi and Y. Takano, *J. Phys. Soc. Jpn.* **79**, 102001 (2010), and references therein.
- ⁶ X. H. Chen, T. Wu, G. Wu, R. H. Liu, H. Chen, and D. F. Fang, *Nature* **453**, 761 (2008).
- ⁷ H. Ding, P. Richard, K. Nakayama, K. Sugawara, T. Arakane, Y. Sekiba, A. Takayama, S. Souma, T. Sato, T. Takahashi, Z. Wang, X. Dai, Z. Fang, G. F. Chen, and J. L. Luo, *Europhys. Lett.* **83**, 47001 (2008).
- ⁸ Y. Nakai, K. Ishida, Y. Kamihara, M. Hirano, and H. Hosono, *J. Phys. Soc. Jpn.* **77**, 073701 (2008).
- ⁹ K. Matano, Z. A. Ren, X. L. Dong, L. L. Sun, Z. X. Zhao, and G. -Q. Zheng, *Europhys. Lett.* **83**, 57001 (2008).
- ¹⁰ C. Martin, R. T. Gordon, M. A. Tanatar, H. Kim, N. Ni, S. L. Bud'ko, P. C. Canfield, H. Luo, H. H. Wen, Z. Wang, A. B. Vorontsov, V. G. Kogan, and R. Prozorov, *Phys. Rev. B* **80**, 020501(R) (2009).
- ¹¹ K. Hashimoto, M. Yamashita, S. Kasahara, Y. Senshu, N. Nakata, S. Tonegawa, K. Ikada, A. Serafin, A. Carrington, T. Terashima, H. Ikeda, T. Shibauchi, and Y. Matsuda *Phys. Rev. B* **81**, 220501(R) (2010).
- ¹² I.I. Mazin, D. J. Singh, M. D. Johannes, and M. H. Du, *Phys. Rev. Lett.* **101**, 057003 (2008).
- ¹³ K. Seo, B.A. Bernevig, and J. Hu, *Phys. Rev. Lett.* **101**, 206404 (2008).
- ¹⁴ K. Kuroki, S. Onari, R. Arita, H. Usui, Y. Tanaka, H. Kontani, and H. Aoki *Phys. Rev. Lett.* **101**, 087004 (2008).
- ¹⁵ V. Cvetkovic, Z. Tesanovic, *Euro. Phys. Lett.* **85**, 37002 (2009).
- ¹⁶ S. Graser, T A Maier, P J Hirschfeld, and D J Scalapino, *New J. Phys.* **11**, 025016 (2009).
- ¹⁷ T. Watanabe, H. Yanagi, T. Kamiya, Y. Kamihara, H. Hiramoto, M. Hirano, and H. Hosono, *Inorg. Chem.* **46**, 7719 (2007).
- ¹⁸ T. Watanabe, H. Yanagi, Y. Kamihara, T. Kamiya, M. Hirano, and H. Hosono, *J. Solid State Chem.* **181**, 2117 (2008).
- ¹⁹ T. Mine, H. Yanagi, T. Kamiya, Y. Kamihara, M. Hirano, and H. Hosono, *Solid State Communications* **147**, 111 (2008).
- ²⁰ H. Fujii and S. Kasahara, *J. Phys.: Condens. Matter* **20**, 075202 (2008).
- ²¹ E. D. Bauer, F. Ronning, B. L. Scott, and J. D. Thompson, *Phys. Rev. B* **78**, 172504 (2008).
- ²² T. Klimczuk, T. M. McQueen, A. J. Williams, Q. Huang, F. Ronning, E. D. Bauer, J. D. Thompson, M. A. Green, and R. J. Cava, *Phys. Rev. B* **79**, 012505 (2009).
- ²³ V. L. Kozhevnikov, O. N. Leonidova, A. L. Ivanovskii, I. R. Shein, B. N. Goshchitskii, and A. E. Karkin, *JETP Lett.* **87**, 649 (2008).
- ²⁴ F. Ronning, N. Kurita, E. D. Bauer, B. L. Scott, T. Park, T. Klimczuk, R. Movshovich, and J. D. Thompson, *J. Phys.: Condens. Matter* **20**, 342203 (2008).
- ²⁵ F. Ronning, E.D. Bauer, T. Park, S.-H. Baek, H. Sakai, and J.D. Thompson, *Phys. Rev. B* **79**, 134507 (2009).
- ²⁶ Z. Li, G. F. Chen, J. Dong, G. Li, W. Z. Hu, D. Wu, S. K. Su, P. Zheng, T. Xiang, N. L. Wang, and J. L. Luo, *Phys. Rev. B* **78**, 060504(R) (2008).
- ²⁷ L. Fang, H. Yang, P. Cheng, X. Zhu, G. Mu, and H. -H. Wen, *Phys. Rev. B* **78**, 104528 (2008).
- ²⁸ F. Ronning, E. D. Bauer, T. Park, N. Kurita, T. Klimczuk, R. Movshovich, A. S. Sefat, D. Mandrus, and J. D. Thompson, *Physica C* **469**, 396 (2009) and references therein.
- ²⁹ A. Subedi and D.J. Singh, *Phys. Rev. B* **78**, 132511 (2008).
- ³⁰ N. Kurita, F. Ronning, Y. Tokiwa, E. D. Bauer, A. Subedi, D. J. Singh, J. D. Thompson, and R. Movshovich, *Phys. Rev. Lett.* **102**, 147004 (2009).
- ³¹ T. Tabuchi, Z. Li, T. Oka, G.F. Chen, S. Kawasaki, J.L. Luo, N.L. Wang, and G.-q. Zheng, *Phys. Rev. B* **81**, 140509 (2010).
- ³² G. Xu, W. Ming, Y. Yao, X. Dai, S.-C. Zhang, and Z. Fang, *Europhys. Lett.* **82**, 67002 (2008).
- ³³ I. R. Shein and A. L. Ivanovskii, *Phys. Rev. B* **79**, 054510 (2009).
- ³⁴ T. Terashima, M. Kimata, H. Satsukawa, A. Harada, K. Hazama, M. Imai, S. Uji, H. Kito, A. Iyo, H. Eisaki, and H. Harima, *J. Phys. Soc. Jpn.* **78**, 033706 (2009).
- ³⁵ J. Lowell and J.B. Sousa, *J. Low. Temp. Phys.* **3**, 65 (1970).
- ³⁶ J. Willis and D. Ginsberg, *Phys. Rev. B* **14**, 1916 (1976).
- ³⁷ M. Sutherland, N. Doiron-Leyraud, L. Taillefer, T. Weller, M. Ellerby, and S. S. Saxena, *Phys. Rev. Lett.* **98**, 067003 (2007).

- ³⁸ S. Y. Li, G. Wu, X.H. Chen, and L. Taillefer, Phys. Rev. Lett. **99**, 107001 (2007).
- ³⁹ A.V. Sologubenko, J. Jun, S.M. Kazakov, J. Karpinski, and H.R. Ott, Phys. Rev. B **66**, 014504 (2002).
- ⁴⁰ E. Boaknin, M.A. Tanatar, J. Paglione, D. Hawthorn, F. Ronning, R.W. Hill, M. Sutherland, L. Taillefer, J. Sonier, S.M. Hayden, and J.W. Brill, Phys. Rev. Lett. **90**, 117003 (2003).
- ⁴¹ M. Suzuki, M.A. Tanatar, N. Kikugawa, Z.Q. Mao, Y. Maeno, T. Ishiguro, Phys. Rev. Lett. **88**, 227004 (2002).
- ⁴² C. Proust, E. Boaknin, R.W. Hill, L. Taillefer, and A.P. Mackenzie, Phys. Rev. Lett. **89**, 147003 (2002).
- ⁴³ R. Marchand, and W. Jeitschko, J. Solid State Chem. **24**, 351 (1978).
- ⁴⁴ See, for example, R. Berman, *Thermal conduction in Solids* (Oxford Univ. Press, Oxford), (1976) and references therein.
- ⁴⁵ N. Kurita, F. Ronning, C. F. Miclea, Y. Tokiwa, E. D. Bauer, A. Subedi, D. J. Singh, H. Sakai, J. D. Thompson, and R. Movshovich, J. Phys.: Conf. ser., in publication.
- ⁴⁶ R. Movshovich, M. A. Hubbard, M. B. Salamon, A. V. Balatsky, R. Yoshizaki, J. L. Sarrao, and M. Jaime, Phys. Rev. Lett. **80**, 1968 (1998).
- ⁴⁷ J. Bardeen, G. Rickayzen, and L. Tewordt, Phys. Rev. **113**, 982 (1959).
- ⁴⁸ A. S. Sefat, M. A. McGuire, B. C. Sales, R. Jin, J. Y. Howe, and D. Mandrus, Phys. Rev. **B 77**, 174503 (2008).
- ⁴⁹ M. Tropeano, A. Martinelli, A. Palenzona, E. Bellingeri, E. Galleani d'Agliano, T. D. Nguyen, M. Affronte, and M. Putti, Phys. Rev. **B 78**, 094518 (2008). M. Tropeano, I. Pallecchi, M. R. Cimberle, C. Ferdeghini, G. Lamura, M. Vignolo, A. Martinelli, A. Palenzona, and M. Putt, Supercond. Sci. Technol. **23**, 054001 (2010).
- ⁵⁰ J. G. Checkelsky, Lu Li, G. F. Chen, J. L. Luo, N. L. Wang, and N. P. Ong, ArXiv: , 0811.4668 (2008).
- ⁵¹ Y. Machida, K. Tomokuni, T. Isono, K. Izawa, Y. Nakajima, T. Tamegai J. Phys. Soc. Japan **78**, 073705 (2009).
- ⁵² K. Krishana, J. M. Harris, and N. P. Ong, Phys. Rev. Lett. **75**, 3529 (1995).
- ⁵³ R. Movshovich, M. Jaime, J. D. Thompson, C. Petrovic, Z. Fisk, P. G. Pagliuso, and J. L. Sarrao, Phys. Rev. Lett. **86**, 5152 (2001).
- ⁵⁴ G.E. Volovik, JETP Lett. **58**, 469 (1993).
- ⁵⁵ S. Nishizaki, Y. Maeno, and Z. Mao, J. Low Temp. Phys. **117**, 1581 (1999).
- ⁵⁶ K. Gofryk, A. S. Sefat, E. D. Bauer, M. A. McGuire, B. C. Sales, D. Mandrus, J. D. Thompson, and F. Ronning, New J. Phys. **12**, 023006 (2010).
- ⁵⁷ K. Gofryk, A. S. Sefat, M. A. McGuire, B. C. Sales, D. Mandrus, J. D. Thompson, E. D. Bauer, and F. Ronning, Phys. Rev. **B 81**, 184518 (2010).
- ⁵⁸ G. Mu, B. Zeng, P. Cheng, Z. Wang, L. Fang, B. Shen, L. Shan, C. Ren, and H. Wen, Chin. Phys. Lett. **27**, 037402 (2010).
- ⁵⁹ F. Hardy, T. Wolf, R. A. Fisher, R. Eder, P. Schweiss, P. Adelmann, H. v. Löehneysen, and C. Meingast, Phys. Rev. **B 81**, 060501(R) (2010).
- ⁶⁰ P. Popovich, A. V. Boris, O. V. Dolgov, A. A. Golubov, D. L. Sun, C. T. Lin, R. K. Kremer, and B. Keimer, Phys. Rev. Lett. **105**, 027003 (2010).
- ⁶¹ M. A. Tanatar, J. P. Reid, H. Shakeripour, X. G. Luo, N. Doiron-Leyraud, N. Ni, S. L. Bud'ko, P. C. Canfield, R. Prozorov, and L. Taillefer Phys. Rev. Lett. **104**, 067002 (2010).
- ⁶² X. G. Luo, M. A. Tanatar, J.-P. Reid, H. Shakeripour, N. Doiron-Leyraud, N. Ni, S. L. Bud'ko, P. C. Canfield, H. Luo, Z. Wang, H.-H. Wen, R. Prozorov, and L. Taillefer Phys. Rev. **B 80**, 140503(R) (2009).
- ⁶³ J. K. Dong, S. Y. Zhou, T. Y. Guan, X. Qiu, C. Zhang, P. Cheng, L. Fang, H. H. Wen, and S. Y. Li Phys. Rev. **B 81**, 094520 (2010).
- ⁶⁴ J. K. Dong, T. Y. Guan, S. Y. Zhou, X. Qiu, L. Ding, C. Zhang, U. Patel, Z. L. Xiao, and S. Y. Li Phys. Rev. **B 80**, 024518 (2009).
- ⁶⁵ M. Yamashita, N. Nakata, Y. Senshu, S. Tonegawa, K. Ikada, K. Hashimoto, H. Sugawara, T. Shibauchi, and Y. Matsuda Phys. Rev. **B 80**, 220509(R) (2009).
- ⁶⁶ J. K. Dong, S. Y. Zhou, T. Y. Guan, H. Zhang, Y. F. Dai, X. Qiu, X. F. Wang, Y. He, X. H. Chen, and S. Y. Li Phys. Rev. Lett. **104**, 087005 (2010).
- ⁶⁷ J.-Ph. Reid, M. A. Tanatar, X. G. Luo, H. Shakeripour, N. Doiron-Leyraud, N. Ni, S. L. Bud'ko, P. C. Canfield, R. Prozorov, and L. Taillefer Phys. Rev. **B 82**, 064501 (2010).
- ⁶⁸ T. Terashima, M. Kimata, H. Satsukawa, A. Harada, K. Hazama, M. Imai, S. Uji, H. Kito, A. Iyo, H. Eisaki, and H. Harima, J. Phys. Soc. Japan **78**, 033706 (2009).
- ⁶⁹ G. Xu, W. Ming, Y. Yao, X. Dai, S.-C. Zhang, and Z. Fang Europhys. Lett. **82**, 094511 (2008).
- ⁷⁰ D.J. Singh, Phys. Rev. **B 78**, 094511 (2008).
- ⁷¹ A.V. Lukoyanov, S.L. Skornyakov, J.A. McLeod, M. Abu-Samak, R.G. Wilks, E. Z. Kurmaev, A. Moewes, N. A. Skorikov, Yu.A. Izyumov, L.D. Finkelstein, V.I. Anisimov, and D. Johrendt, Phys. Rev. **B 81**, 235121 (2010).
- ⁷² Q. Tao, Z. Zhu, X. Lin, G. Cao, Z.-a. Xu, G. Chen, J. Luo, and N. Wang, J. Phys.: Condens. Matter **22**, 072201 (2010).
- ⁷³ Z. G. Chen, G. Xu, W. Z. Hu, X. D. Zhang, P. Zheng, G. F. Chen, J. L. Luo, Z. Fang, and N. L. Wang, Phys. Rev. **B 80**, 094506 (2009).
- ⁷⁴ Y. Nakai, K. Ishida, Y. Kamihara, M. Hirano, and H. Hosono, Phys. Rev. Lett **B 101**, 077006 (2008).
- ⁷⁵ C. P. Bean, Phys. Rev. Lett. **8**, 250 (1962); Rev. Mod. Phys. **36**, 31 (1964).